APPLIED AND ENVIRONMENTAL MICROBIOLOGY, Nov. 2002, p. 5274–5280 Vol. 68, No. 11
0099-2240/02/$04.00+0 DOI: 10.1128/AEM.68.11.5274–5280.2002

Mode of Action of the Antimicrobial Peptide Aureocin A53 from *Staphylococcus aureus*

Daili Jacqueline Aguilar Netz,[1,2] Maria do Carmo de Freire Bastos,[1] and Hans-Georg Sahl[2]*

Departamento de Microbiologia Geral, Instituto de Microbiologia, Universidade Federal do Rio de Janeiro, Rio de Janeiro, Brazil,[1]; and Institut für Medizinische Mikrobiologie und Immunologie, Universität Bonn, Bonn, Germany[2]

Received 21 March 2002/Accepted 5 August 2002

We investigated the mode of action of aureocin A53 on living bacterial cells and model membranes. Aureocin A53 acted bactericidally against *Staphylococcus simulans* 22, with >90% of the cells killed within a few minutes. Cell death was followed by lysis, as indicated by a clearing of the cell suspension and Gram staining. Aureocin A53 rapidly dissipated the membrane potential and simultaneously stopped biosynthesis of DNA, polysaccharides, and protein. Aureocin A53 induced a rapid release of preaccumulated glutamate and Rb^+. Experiments on model membranes demonstrated that aureocin A53 provoked significant leakage of carboxyfluorescein (CF) exclusively from acidic liposomes but only at relatively high concentrations (0.5 to 8 mol%). Thus, the bactericidal activity of aureocin A53 derives from membrane permeation via generalized membrane destruction rather than by formation of discrete pores within membranes. Tryptophan emission fluorescence spectroscopy demonstrated interaction of aureocin A53 with both acidic and neutral membranes, as indicated by similar blue shifts. Since there was no significant aureocin A53-induced CF leakage from neutral liposomes, its appears that the peptide does interact with neutral lipids without provoking membrane damage.

During the past decade, a plethora of antimicrobial cationic peptides have been isolated from a range of organisms, including animals, plants, insects, and bacteria (13). The bacteriocins constitute a large family of antimicrobial agents that vary greatly in size and primary sequence but tend to be small cationic peptides of 20 to 60 amino acids with amphipathic characteristics and high isoelectric points (11, 16, 28). Class I bacteriocins are modified peptides, lantibiotics, which contain lanthionine residues forming intramolecular rings. The peptides generally have a broad spectrum of activity and form unstable pores. Docking molecules may enhance the conductivity and stability of lantibiotic pores (5, 6, 31). Class II bacteriocins are small heat-stable peptides, most with a narrow spectrum of activity, and act primarily by membrane permeabilization of susceptible microorganisms (11); again, specific targets may be involved in the activity, such as the mannose-specific PTS protein in the pediocin family of bacteriocins (8, 9, 23).

We have recently described a new nonlantibiotic bacteriocin isolated from *Staphylococcus aureus*, aureocin A53 (21), which shares some physicochemical characteristics with class II bacteriocins. Aureocin A53 is a tryptophan-rich 51-residue peptide and has a net charge of 8+ and an amphiphilic nature. Unlike most class II bacteriocins, aureocin A53 is synthesized without a leader peptide and retains a formylated N terminus. Consequently, genes for biosynthetic enzymes, immunity functions, or regulation of biosynthesis are not found in the vicinity of the aureocin A53 structural gene. Remarkably, an ordered structure in aqueous solution consisting of 36% ± 5% helical and 18% ± 4% β-sheet conformation was observed by circular-dichroism spectroscopy (21). The present study characterizes the in vivo mode of action of aureocin A53 on *Staphylococcus simulans* 22 through killing kinetics and assessment of its effect on the incorporation and efflux of radiolabeled substances and membrane potential. We also describe its interaction with artificial membranes of different phospholipid compositions by carboxyfluorescein (CF) efflux measurements and fluorescence spectroscopy of the intrinsic tryptophan residues of aureocin A53. Our data suggest that the bactericidal activity of aureocin A53 derives from generalized membrane permeabilization rather than from the formation of defined or target-mediated pores.

* Corresponding author: Mailing address: Institut für Medizinische Mikrobiologie und Immunologie der Universitat Bonn, Sigmund-Freud-Str. 25, 53105 Bonn, Germany. Phone: 49 228 287 5704. Fax: 49 228 287 4808. E-mail: sahl@mibi03.meb.uni-Bonn.de.

MATERIALS AND METHODS

Bacterial strains and culture conditions. The bacteriocin-producing strain *S. aureus* A53 was previously isolated from pasteurized commercial milk (12). The strains used as indicator microorganisms are listed in Table 1. Stock cultures were stored in tryptone soy broth (Oxoid) at −70°C as 40% glycerol suspensions. Working cultures were maintained on Trypticase soy agar plates and subcultured weekly at 37°C

Purification of aureocin A53 and antimicrobial activity assays. Purification of aureocin A53 was performed according to the method of Netz et al. (21). The purity of aureocin A53 was confirmed by analytical high-performance liquid chromatography and matrix-assisted laser desorption ionization–time of flight mass spectrometry. The minimal growth-inhibitory concentrations of aureocin A53 for the indicator strains and some gram-positive microorganisms (Table 1) were determined by the broth microdilution method in microtiter plates. Serial twofold dilutions of purified aureocin A53 were prepared in half-concentrated Mueller-Hinton broth (Oxoid). Bacteria in the exponential growth phase were added to give a final inoculum of 10^5 CFU/ml in a total volume of 0.2 ml. After incubation for 16 h at 37°C, the lowest concentration of the antimicrobial agent resulting in inhibition of growth (MIC) was determined.

Bacterial killing assay. Overnight cultures of the indicator strain *S. simulans* 22 were diluted 100-fold in half-concentrated Mueller-Hinton broth and allowed

TABLE 1. MICs of aureocin A53 for various gram-positive bacteria

Organism	Strain	Description	MIC (μg/ml)	Reference
E. faecium	BM4147	Vancomycin resistant	0.29	17
L. innocua	ATCC 33090	Apathogenic	0.59	
M. luteus	ATCC 4698	Aureocin A53 sensitive	0.87×10^{-3}	
S. aureus	LT-1334[a]	Methicillin-resistant isolate	1.17	
S. aureus	J-11574[a]	Methicillin-susceptible isolate	1.17	
Staphylococcus epidermidis	LT-1324[a]	Methicillin-resistant isolate	0.59	
S. simulans 22		Aureocin A53 sensitive	0.59	26

[a] Strain isolated in the Institute for Medical Microbiology and Immunology of the University Bonn, Bonn, Germany.

to grow to the mid-exponential phase (A_{600}, 0.4) at 37°C. Aureocin A53 was added at a concentration equal to or 10-fold higher than the MIC (0.59 and 5.9 μg/ml, respectively), and samples were removed at regular intervals to determine the optical density at 600 nm, appropriately diluted, and plated onto Mueller-Hinton agar plates to obtain viable cell counts.

Incorporation and efflux of radioactive metabolites. The effect of aureocin A53 on the synthesis of macromolecules was studied by recording the incorporation of ^{3}H-labeled precursors (glucose, glutamate, and thymidine) and the efflux of glutamate according to the method described by Sahl and Brandis (26, 27), with some modifications introduced by Ruhr and Sahl (25). For glutamate efflux experiments, cells were preincubated with 100 μg of chloramphenicol (Sigma)/ml to inhibit protein synthesis. Aureocin A53 was used at 10 times the MIC. For $^{86}Rb^+$ efflux, the protocol was adapted as follows. After overnight growth on PYG medium (0.5% Bacto Peptone [Merck]–0.4% glucose [Merck]–0.4% yeast extract [Merck] buffered with 10 mM Tris-HCl, pH 7), the cells were diluted in fresh medium to an A_{600} of 0.05. $^{86}Rb^+$ was added (0.5-μCi/ml cell suspension), and the cell suspension was allowed to grow at 37°C to an A_{600} of 1.0 with shaking. Before and after the addition of aureocin A53 (at 1 and 10 times the MIC), samples were removed at regular intervals and filtered on 0.2-μm-pore-size membrane filters (Schleicher & Schuell, Dassel, Germany) as described previously (26). All radioisotopes were purchased from Amersham-Pharmacia (Braunschweig, Germany).

Membrane potential estimation. *S. simulans* 22 was grown on PYG medium buffered with 100 mM phosphate buffer, pH 7, at 37°C to an optical density at 600 nm of 0.4. The cells were centrifuged, suspended in fresh PYG medium, and incubated at 37°C under agitation. The culture was divided into four equal parts. Three were treated with aureocin A53 (at 0.1, 1.0, and 10 times the MIC), and the other was run as a control. The experiment was started by the addition of 0.2 μCi of [^{3}H]tetraphenylphosphonium (TTP^+) (Amersham Pharmacia) per ml of cell suspension. Aliquots were filtered on 0.2-μm-pore-size cellulose acetate membranes (Schleicher & Schuell) and washed with 50 mM phosphate buffer, pH 7.0. The filters were dried and the radioactivity was counted in 5 ml of Quickszint 100 (Zinsser Analytic; Berkshire, United Kingdom) in a Packard 1900 CA liquid scintillation counter. $\Delta\Psi$ was calculated as described by Ruhr and Sahl (25) using the Nernst equation ($\Delta\psi = -2.3 \times R \times T/F \times \log TTP^+_{in}/TTP^+_{out}$, where $\Delta\Psi$ is membrane potential, R is the gas constant, T is absolute temperature (in Kelvins), F is the Farraday constant, TPP^+_{in} is TPP^+ inside the cells, and TPP^+_{out} is TPP^+ outside the cells). The counts were corrected for nonspecific TTP^+ binding to cell constituents by subtracting the counts obtained for control cells treated with 10% butanol.

CF leakage experiments. Large unilamellar vesicles for CF efflux were prepared by the extrusion method (15) and treated as previously described (4). The vesicles were made of 1,2-diacyl-SN-glycero-3 phosphocholine (DOPC); 1,2-diacyl-SN-glycero-3[phospho-*Rac*-(1-glycerol)] (DOPG), and DOPC-DOPG (1:1) (all from Avanti Polar Lipids). Phospholipid concentrations were quantified as inorganic phosphate after treatment with perchloric acid (24). CF-loaded vesicles were prepared in the presence of 50 mM CF, and the extravesicular CF was removed by gel filtration (Sephadex G-25; Pharmacia) and then diluted with 50 mM MES (morpholineethanesulfonic acid)-KOH (pH 6.0)–100 mM K_2SO_4 to a final concentration of 25 μM phospholipid. The solution was kept at 20°C and continuously stirred. After the addition of various concentrations of aureocin A53, the induced leakage was monitored for 3 min. The fluorescence increase (decrease of self-quenching) was measured at 515 nm (excitation at 492 nm) with an SPF 500C spectrophotometer (SLM instruments Inc.) at 20°C. The aureocin A53-induced CF leakage was expressed relative to the total amount of CF released after disruption of the vesicles by the addition of 10 μl of 20% Triton X-100.

Emission spectra and intensity measurements. Tryptophan fluorescence emission spectra were recorded in 50 mM MES-KOH (pH 6.0)–100 mM K_2SO_4 using an SPF 500C spectrophotometer. Emission spectra were recorded from 300 to 500 nm (bandwidth, 5 nm) with excitation at 280 nm (bandwidth, 5 nm). The solution in the cuvette was kept at 20°C and continuously stirred. Aureocin A53 was used at a concentration of 1.0 μM in the absence or presence of vesicles composed of DOPC, DOPC-DOPG (1:1), and DOPG at a concentration of 25 μM lipid-P_i. The absorbance of vesicles and aureocin A53 at 280 nm was lower than 0.05. Spectra were corrected for background fluorescence of the lipids (<10% at all emission wavelengths).

RESULTS

Antimicrobial activity. The MICs of aureocin A53 for a range of gram-positive bacteria are given in Table 1. For *Listeria innocua* and staphylococci, including coagulase-negative strains, as well as methicillin-sensitive and methicillin-resistant *S. aureus* strains, the MICs were in the range of 1 μg/ml. The MIC for a vancomycin-resistant strain of *Enterococcus faecium*, a pathogen with prominent antibiotic resistance development, was 0.29 μg/ml. Consistent with many antimicrobial agents, the most sensitive strain was *Micrococcus luteus*, for which the MIC was only 0.87 ng/ml. In control experiments with the well-characterized indicator strain *S. simulans* 22 in which the microtiter plates were precoated with bovine serum albumin, it was noticed that the MIC decreased 10-fold. Apparently, undesirable interaction of the polypropylene matrix with the highly cationic aureocin A53 reduced the bioavailability of the bacteriocin at low concentrations. Since for most experiments described in this study precoating of culture flasks was not feasible, we refer to the MIC obtained without precoating.

Bacterial killing assays. The effects of aureocin A53 on the viability of exponentially growing *S. simulans* 22 cells (5×10^7 CFU/ml) were tested at 1 and 10 times the MIC (Fig. 1). Five minutes after the addition of 10 times the MIC, the number of surviving cells was drastically reduced to 0.02%; after 60 min, it was reduced to 0.002%; and after 6 h, it was reduced to 2×10^{-5}%(data not shown), whereas at the MIC, the number of surviving cells was reduced to 6, 0.1, and 2×10^{-4}% (data not shown), respectively. Thus, aureocin A53 has an immediate dose-dependent killing effect. A gradual decrease in the optical density at 600 nm from 0.40 to 0.11 after 6 h was observed at both tested concentrations (data not shown). Gram staining showed that, in parallel with loss of viability, the number of stainable cells decreased, indicating the rapid onset of a cell wall-lytic process. Such a phenomenon has been described for *S. simulans* 22 when treated with the cationic peptide Pep5 or nisin (2, 3), for which it was shown that the peptides displaced,

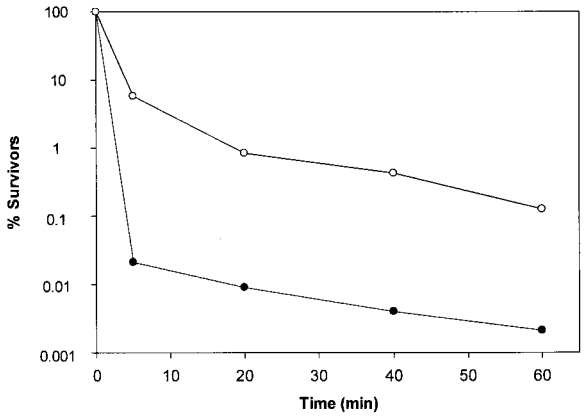

FIG. 1. Killing kinetics of *S. simulans* 22 by aureocin A53 in half-concentrated Mueller-Hinton broth at 37°C. Shown is the percent survival of cells after the addition of 5.9 (●) or 0.59 (○) μg of aureocin A53/ml.

and thereby activated, cell wall-lytic enzymes from anionic polymers (teichoic and lipoteichoic acids).

Inhibition of macromolecular synthesis and membrane depolarization. Rapid killing is a characteristic feature of cationic membrane-disintegrating agents. To verify the effect of aureocin A53 on bacterial membranes, macromolecular synthesis assays were performed with *S. simulans* 22 in the presence of 10 times the MIC. Addition of aureocin A53 to exponentially growing cells of *S. simulans* 22 immediately blocked the incorporation of [^{3}H]glucose, [^{3}H]thymidine, and [^{3}H]glutamate into the acid-precipitable cell fraction (Fig. 2). Thus, the macromolecular synthesis of polysaccharide, DNA, and proteins ceased simultaneously. Since these processes are dependent on energy and the availability of metabolic precursors, it appears likely that blockage of these processes occurred via leakage of essential molecules and dissipation of the membrane potential.

In fact, aureocin A53 depolarized cells at the same rate as killing (Fig. 3) and inhibition of biosynthetic processes occurred, indicating that the dissipation of $\Delta\Psi$ and killing are directly linked. Even at 10 times the MIC, depolarization appeared to be incomplete, probably reflecting the fact that under the experimental conditions necessary for conducting $\Delta\Psi$ measurements, e.g., the presence of 10^8 to 10^9 cells/ml, a significant number of surviving cells are still present (in accordance with killing kinetics [Fig. 1]). Consequently, at 0.1 MIC, significantly fewer cells were affected. Additionally, at this low concentration, some recuperation of the potential was observed, indicating that individual cells may recover from the bacteriocin action and restore the membrane potential.

Efflux experiments. The influence of aureocin A53 on the accumulation and efflux of [^{3}H]glutamate was tested in experiments in which protein synthesis was blocked with chloramphenicol. In accordance with the kinetics of membrane depolarization, the addition of aureocin A53 at 10 times the MIC induced a rapid efflux of 40% of the [^{3}H]glutamate in the first 30 s (Fig. 4A). Within 2 min, 70% efflux was observed, and after 5 min, the radioactivity decreased to a basal level. Compared to that of glutamate, efflux of the potassium ion analogue $^{86}Rb^+$ was considerably faster. The question of whether this reflects ion selectivity of the pore (net negatively charged

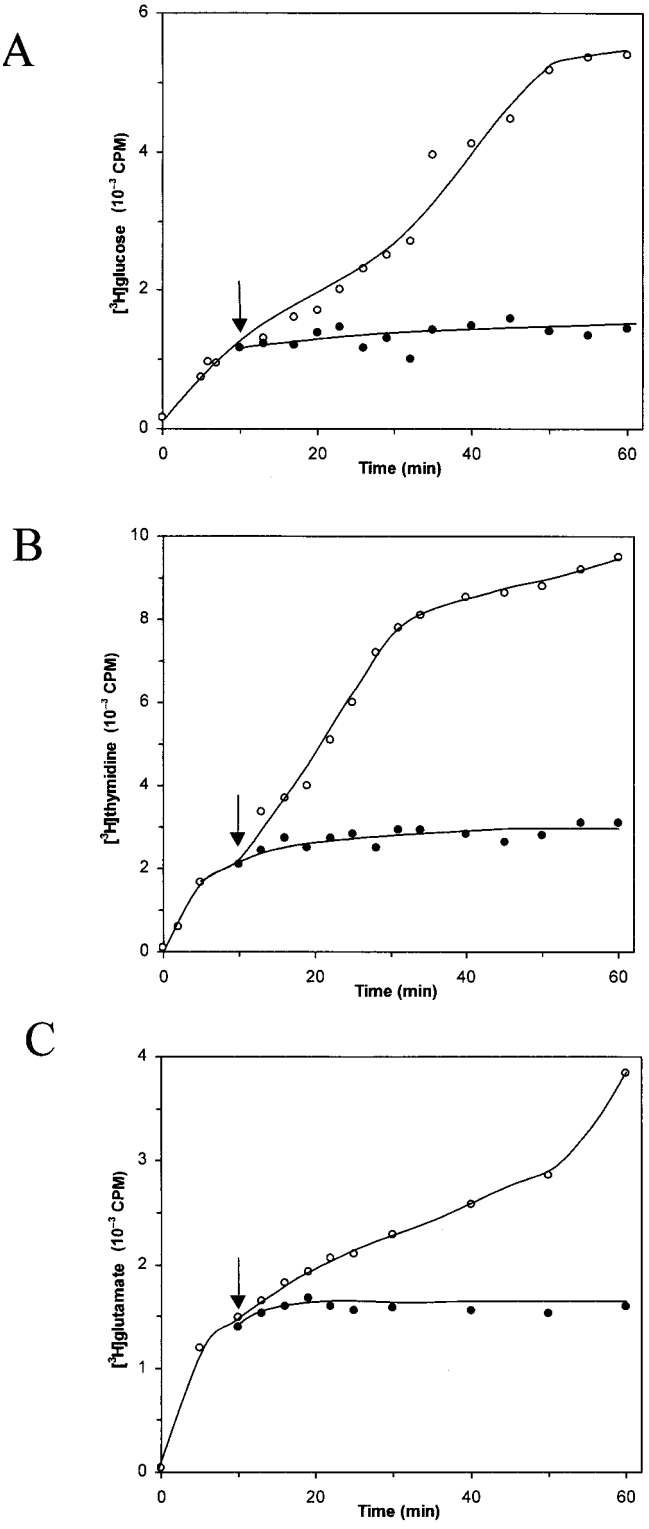

FIG. 2. Influence of aureocin A53 on macromolecular synthesis (indicator strain, *S. simulans* 22). Shown is the uptake of [^{3}H]glucose (A), [^{3}H]thymidine (B), and [^{3}H]glutamate (C) into the cellular macromolecules by *S. simulans* 22. ○, untreated cells; ●, cells treated with aureocin A53 at 10 times the MIC. The arrows indicate the points of addition of bacteriocin.

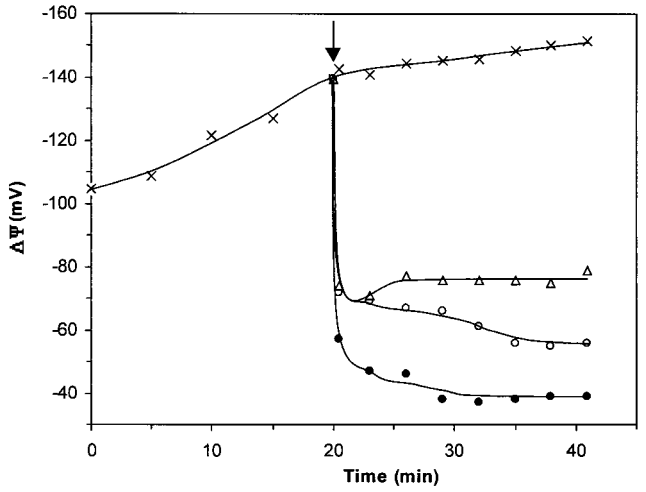

FIG. 3. Effect of aureocin A53 on membrane potential of *S. simulans* 22. ×, control without bacteriocin; △, aureocin A53 at 0.1 MIC; ○, aureocin A53 at MIC; ●, aureocin A53 at 10 times MIC. The arrow indicates the moment of addition of aureocin A53.

compound versus inorganic cation) or whether it is due to the different M_rs of the test compounds and thus indicates pores of finite size remains to be studied.

Activity on artificial liposomes. The interaction of aureocin A53 with unilamellar liposomes of different lipid compositions (DOPC, DOPC-DOPG [1:1], and DOPG) was studied by CF efflux assays (Fig. 5). The addition of aureocin A53 to liposomes with a negative surface charge (i.e., DOPG and DOPC-DOPG mixtures) caused an immediate and rapid efflux of CF followed by a period of slower dye release. In contrast, liposomes composed solely of the zwitterionic and net neutral DOPC were weakly affected by the bacteriocin (Fig. 5). We used the percentage of efflux reached after 2 min for a closer inspection of the concentration dependence of the aureocin A53 membrane poration (Fig. 6). Obviously, relatively high peptide-to-lipid molar ratios (0.5 to 8 mol%) were necessary to induce substantial efflux from DOPG-containing liposomes. For DOPC liposomes, even at 8 mol% only a marginal efflux activity was detectable.

Tryptophan fluorescence spectroscopy. Aureocin A53 has five intrinsic tryptophan residues, which enables the use of fluorescence spectroscopy to study the interaction of peptides with different membranes. The fluorescence emission spectra of aureocin A53 in buffer and in the presence of liposomes with different phospholipid compositions are shown in Fig. 7. In buffer, aureocin A53 showed a fluorescence emission maximum of approximately 350 nm, which is characteristic of tryptophan residues in a polar environment (30). The addition of aureocin A53 (4 mol%) to DOPC and DOPC-DOPG (1:1) liposomes induced a net blue shift of the emission maximum of 10 nm, as well as an increase in fluorescence (Fig. 7). In general, a blue shift is accompanied by an increased fluorescence quantum yield and is indicative of a more hydrophobic environment of the tryptophan side chains. With negatively charged DOPG liposomes, the emission maximum shifted by only 5 nm and the increase in fluorescence was smaller than with DOPC-containing membranes. It is reasonable to assume

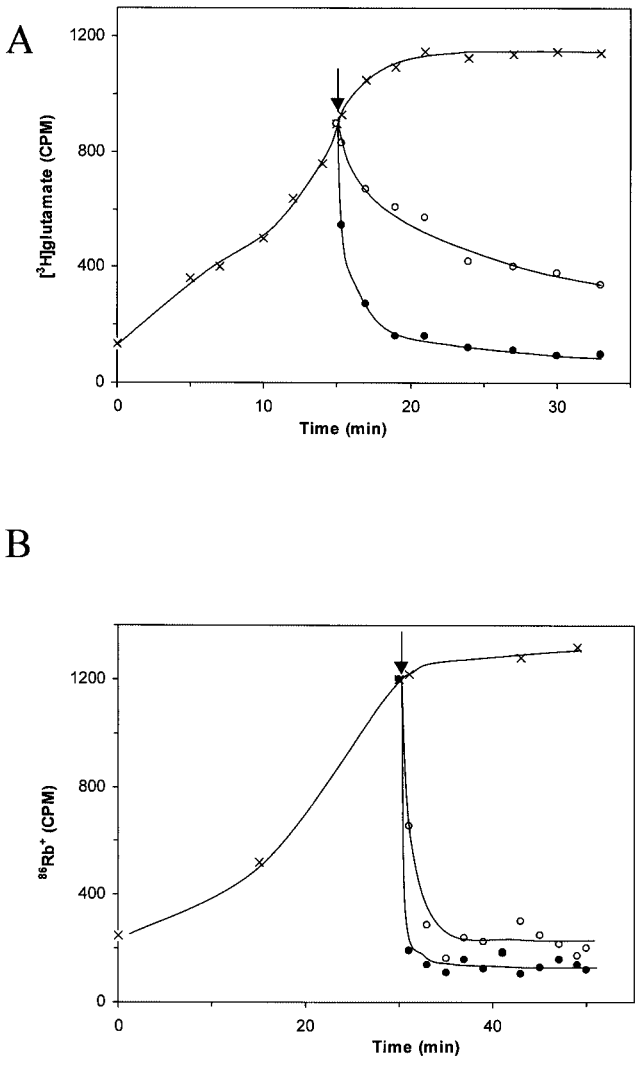

FIG. 4. (A) Accumulation of [^{3}H]glutamate by *S. simulans* 22 (×) and efflux upon addition of aureocin A53 at MIC (○) and 10 times MIC (●). (B) Accumulation of $^{86}Rb^+$ by *S. simulans* 22 (×) and efflux of $^{86}Rb^+$ upon addition of aureocin A53 at MIC (○) and 10 times MIC (●). The arrows indicate the addition of peptide.

that aureocin A53, at least partially, inserts into the membrane. Interestingly, and in contrast to what was expected from the dye release experiments, the interactions with DOPC and DOPC-DOPG appeared to be more pronounced than those with DOPG liposomes.

DISCUSSION

In the present work, we demonstrate that aureocin A53 primarily acts by permeabilization of the cell membrane followed by efflux of vital compounds, dissipation of the membrane potential, and cessation of macromolecular synthesis. Aureocin A53 interacted with neutral and acidic membranes, inducing similar fluorescence blue shifts, but preferentially induced leakage from acidic liposomes. Since aureocin A53 requires micromolar concentrations to kill bacteria and induce efflux from cells and negatively charged liposomes, it is likely to

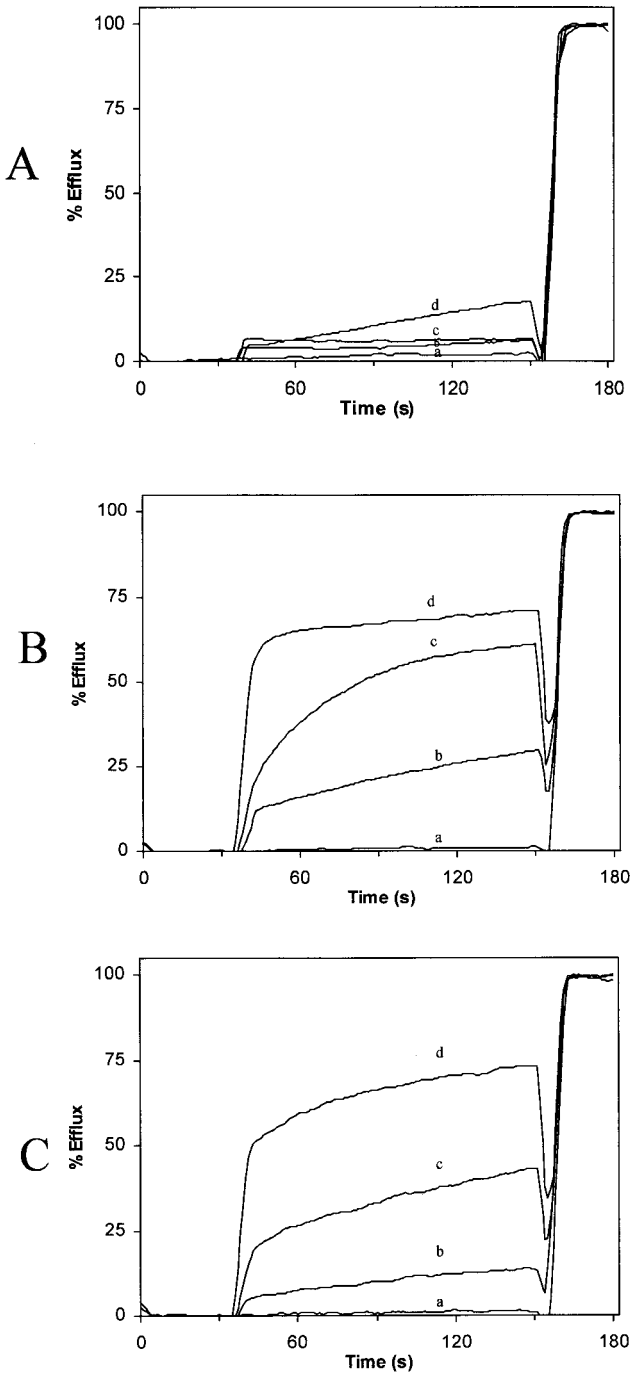

FIG. 5. CF leakage from DOPC (A), DOPC-DOPG (1:1) (B), and DOPG (C) liposomes after addition of different concentrations of aureocin A53 (a, 0.0 μM; b, 0.25 μM; c, 1.0 μM; d, 2.0 μM).

produce membrane permeabilization through generalized membrane disruption rather than through formation of defined pores.

Various models for membrane permeabilization by antimicrobial peptides have been postulated. While alamethicin may form pores according to the barrel stave mechanism (7, 14, 19), magainin is postulated to form thoroidal pores (18). Taking into account the high concentration necessary to produce membrane leakage, a more generalized carpeting and subsequent disruption of the membrane was proposed for other groups of peptides (22). Recently, Zasloff (33) merged several proposed mechanisms into one general model, the SMH (Shai-Matsuzaki-Huang) model (20, 29, 32). This model proposes the interaction of the peptide with the membrane, followed by displacement of lipids, alteration of membrane structure, and, in certain cases, entry of the peptide into the interior of the target cell. The peptides that work according to the SMH model kill microorganisms at micromolar concentrations, i.e., in the same range of concentration which is necessary to produce effects on model membranes, supporting the view that in vivo the microbial membrane is the primary target of their antibiotic action. In contrast nisin, a lantibiotic peptide, acts in the nanomolar range by binding with high affinity to the membrane-bound cell wall precursor lipid II, using it as a docking molecule for target-mediated pore formation and simultaneously blocking its incorporation into peptidoglycan (6, 31). Additionally, at micromolar concentration, it acts according to the SMH model (5). Therefore, activity in the nanomolar

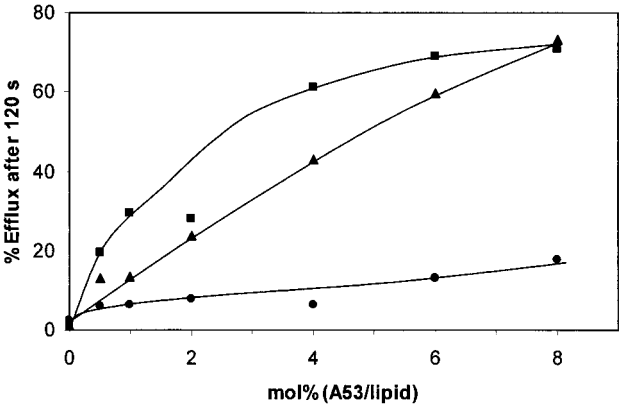

FIG. 6. Relationship between rate of CF release and molar ratio of peptide per lipid after addition of DOPC (●), DOPC-DOPG (1:1) (■), and DOPG (▲) liposomes.

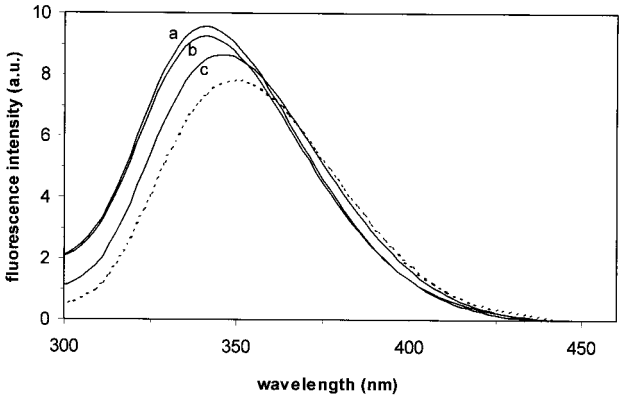

FIG. 7. Fluorescence emission spectrum of 1 μM aureocin A53 in the presence of 25 μM DOPC-DOPG (1:1) (tracing a), DOPC (tracing b), and DOPG (tracing c) liposomes (lipid-P_i) or in the absence of lipids (dotted line). a.u., arbitrary units.

range may indicate highly effective target pore formation, which has also been observed for class IIa bacteriocins active against *Listeria monocytogenes* (10). In that case, the mannose-specific PTS protein is involved in sensitivity to *L. monocytogenes* and *Enterococcus faecalis*, and it could represent a docking molecule for the type IIa bacteriocin family (1, 8, 9, 23).

Our experiments on whole cells and artificial liposome membranes showed that aureocin A53 acts on both in micromolar concentrations, suggesting that it operates according to the SMH model and that specific targets may not be involved. The interaction of aureocin A53 with the cytoplasmic membrane then leads to efflux of vital components and dissipation of the membrane potential of cells and simultaneously stops cell macromolecular synthesis. Independent of membrane depolarization, the rapid onset of autolysins may significantly contribute to the microbicidal activity of aureocin A53. The induction of autolysins may be due to displacement of the enzymes from anionic wall polymers, as was described in detail for the cationic peptides Pep5 and nisin (2, 3).

For peptides acting as proposed by the SMH model, it is generally assumed that the ionic interaction between the cationic peptides and the negatively charged phospholipids is important for the initial binding, which then leads to structuring of peptides into the characteristic amphiphilic shape, insertion of the hydrophobic portion of the peptides into the membrane bilayer, and subsequent physical destabilization and membrane disruption. Our results with liposomes suggest that for aureocin A53 the situation may be significantly different. Previous data on the structure of the peptide (21) clearly indicated that in aqueous solution, it has a defined, rigid structure and that the five Trp residues are likely located on the surface of the molecule. The tryptophan fluorescence studies conducted here clearly show that, even in the absence of a negatively charged membrane surface, aureocin A53 binds to the membrane, possibly even more strongly to neutral membranes than to the negatively charged phospholipids (DOPG), as indicated by the stronger blue shift and the fluorescence increase obtained with DOPC liposomes. Interestingly, the interaction with DOPC hardly provokes membrane disruption and CF leakage (Fig. 5). This raises questions as to the importance of charged lipids for peptides to induce membrane disruption rather than for initial binding of the peptide to the membrane surface. Future studies will address these questions and reveal whether this may be of general importance for cationic amphiphilic peptides, whether it is relevant only for those which are structured in aqueous solutions, e.g., the α and β defensins, or whether it is a unique feature of aureocin A53.

ACKNOWLEDGMENTS

This study was supported by grants from FAPERJ and FUJB (Brazil) to Maria do Carmo de Freire Bastos. Daili Jacqueline Aguilar Netz is the recipient of a fellowship from CAPES/DAAD and was supported by a BONFOR laboratory grant of the Medical Faculty, University of Bonn.

We greatly appreciate the general help of group members with various techniques and thank Antonio Pierik, Philipps University, Marburg, Germany, for help with the manuscript and for support.

REFERENCES

1. **Bennik, M. H. J., B. Vanloo, R. Brasseur, L. G. M. Gorris, and E. J. Smid.** 1998. A novel bacteriocin with a YGNGV motif from vegetable-associated *Enterococcus mundtii*: full characterization and interaction with target organisms. Biochem. Biophys. Acta **1373:**47–58.
2. **Bierbaum, G., and H.-G. Sahl.** 1985. Induction of autolysis of staphylococci by the basic peptide antibiotics Pep 5 and nisin and their influence on the activity of autolytic enzymes. Arch. Microbiol. **141:**249–254.
3. **Bierbaum, G., and H.-G. Sahl.** 1987. Autolytic system of *Staphylococcus simulans* 22: influence of cationic peptides on activity of *N*-acetylmuramoyl-L-alanine amidase. J. Bacteriol. **169:**5452–5458.
4. **Breukink, E., C. van Kraaij, R. A. Demel, R. J. Siezen, O. P. Kuipers, and B. de Kruijff.** 1997. The C-terminal region of nisin is responsible for the initial interaction of nisin with the target membrane. Biochemistry **36:**6968–6976.
5. **Breukink, E., I. Wiedemann, C. van Kraaij, O. P. Kuipers, H.-G. Sahl, and B. de Kruijff.** 1999. Use of the cell wall precursor lipid II by a pore-forming peptide antibiotic. Science **286:**2361–2364.
6. **Brötz, H., G. Bierbaum, K. Leopold, P. E. Reynolds, and H.-G. Sahl.** 1998. The lantibiotic mersacidin inhibits peptidoglycan synthesis by targeting lipid II. Antimicrob. Agents Chemother. **42:**154–160.
7. **Chen, F. Y., M. T. Lee, and H. W. Huang.** 2002. Sigmoidal concentration dependence of antimicrobial peptide activities: a case study on alamethicin. Biophys. J. **82:**908–914.
8. **Dalet, K., C. Briand, Y. Cenatiempo, and Y. Hechard.** 2000. The *rpoN* gene of *Enterococcus faecalis* directs sensitivity to subclass IIa bacteriocins. Curr. Microbiol. **41:**441–443.
9. **Dalet, K., Y. Cenatiempo, P. Cossart, and Y. Hechard.** 2001. A sigma(54)-dependent PTS permease of the mannose family is responsible for sensitivity of *Listeria monocytogenes* to mesentericin Y105. Microbiology **147:**3263–3269.
10. **Eijsink, V. G. H., M. Skeie, P. H. Middelhoven, M. B. Brurberg, and I. F. Nes.** 1998. Comparative studies of class IIa bacteriocins of lactic acid bacteria. Appl. Environ. Microbiol. **64:**3275–3281.
11. **Ennahar, S., T. Sashihara, K. Sonomoto, and A. Ishizaki.** 2000. Class IIa bacteriocins: biosynthesis, structure and activity. FEMS Microbiol. Rev. **24:** 85–106.
12. **Giambiagi-deMarval, M., M. A. Mafra, E. C. G. Penido, and M. C. F. Bastos.** 1990. Distinct groups of plasmids correlated with bacteriocin production in *Staphylococcus aureus*. J. Gen. Microbiol. **136:**1591–1599.
13. **Hancock, R. E., T. Falla, and M. Brown.** 1995. Cationic bactericidal peptides. Adv. Microb. Physiol. **37:**135–175.
14. **He, K., S. J. Ludtke, D. L. Worcester, and H. W. Huang.** 1996. Neutron scattering in the plane of membranes: structure of alamethicin pores. Biophys. J. **70:**2659–2666.
15. **Hope, M. J., M. B. Bally, G. Webb, and P. R. Cullis.** 1985. Production of large unilamellar vesicles by a rapid extrusion procedure. Characterization of size distribution, trapped volume and ability to maintain a membrane potential. Biochim. Biophys. Acta **812:**55–65.
16. **Jack, R. W., J. R. Tagg, and B. Ray.** 1995. Bacteriocins of Gram-positive bacteria. Microbiol. Rev. **59:**171–200.
17. **Leclercq, R., E. Derlot, J. Duval, and P. Courvalin.** 1988. Plasmid-mediated resistance to vancomycin and teicoplanin in *Enterococcus faecium*. N. Engl. J. Med. **319:**157–161.
18. **Ludtke, S. J., K. He, W. T. Heller, T. A. Harroun, L. Yang, and H. W. Huang.** 1996. Membrane pores induced by magainin. Biochemistry **35:**13723–13728.
19. **Mak, D. O., and W. W. Webb.** 1995. Molecular dynamics of alamethicin transmembrane channels from open-channel current noise analysis. Biophys. J. **69:**2337–2349.
20. **Matsuzaki, K.** 1999. Why and how are peptide-lipid interactions utilized for self-defense? Magainins and tachyplesins as archetypes. Biochim. Biophys. Acta **1462:**1–10.
21. **Netz, D. J. A., R. Pohl, A. G. Beck-Sickinger, T. Selmer, A. J. Pierik, M. C. F. Bastos, and H.-G. Sahl.** 2002. Biochemical characterization and genetic analysis of aureocin A53, a new, atypical bacteriocin from *Staphylococcus aureus.* J. Mol. Biol. **319:**745–756.
22. **Oren, Z., and Y. Shai.** 1998. Mode of action of linear amphipathic alpha-helical antimicrobial peptides. Biopolymers **47:**451–463.
23. **Ramnath, M., M. Beukes, K. Tamura, and J. W. Hastings.** 2000. Absence of a putative mannose-specific phosphotransferase system enzyme IIAB component in a leucocin A-resistant strain of *Listeria monocytogenes*, as shown by two-dimensional sodium dodecyl sulfate-polyacrylamide gel electrophoresis. Appl. Environ. Microbiol. **66:**3098–3101.
24. **Rouser, G., S. Fleischer, and A. Yamamoto.** 1970. Two dimensional thin layer chromatographic separation of polar lipids and determination of phospholipids by phosphorus analysis of spots. Lipids **5:**494–496.
25. **Ruhr, E., and H.-G. Sahl.** 1985. Mode of action of the peptide antibiotic nisin and influence on the membrane potential of whole cells and on cytoplasmic and artificial membrane vesicles. Antimicrob. Agents Chemother. **27:**841–845.
26. **Sahl, H.-G., and H. Brandis.** 1982. Mode of action of the staphylococcin-like peptide Pep5 and culture conditions affecting its activity. Zentbl. Bakteriol. Mikrobiol. Hyg. A **252:**166–175.
27. **Sahl, H.-G., and H. Brandis.** 1983. Efflux of low-M_r substances from the cytoplasm of sensitive cells caused by the staphylococcin-like agent Pep5. FEMS Microbiol. Lett. **16:**75–79.
28. **Sahl, H.-G., and G. Bierbaum.** 1998. Lantibiotics: biosynthesis and biological

activities of uniquely modified peptides from gram-positive bacteria. Annu. Rev. Microbiol. **52:**41–79.
29. **Shai, Y.** 1999. Mechanism of the binding, insertion and destabilization of phospholipid bilayer membranes by α-helical antimicrobial and cell nonselective membrane-lytic peptides. Biochem. Biophys. Acta **1462:**55–70.
30. **Surewicz, W. K., and R. M. Epand.** Role of peptide structure in lipid-peptide interactions: a fluorescence study of the binding of pentagastrin-related pentapeptides to phospholipid vesicles. Biochemistry **23:**6072–6077.
31. **Wiedemann, I., E. Breukink, C. van Kraaij, O. P. Kuipers, G. Bierbaum, B. de Kruijff, and H.-G. Sahl.** 2001. Specific binding of nisin to the peptidoglycan precursor lipid II combines pore formation and inhibition of cell wall biosynthesis for potent antibiotic activity. J. Biol. Chem. **276:**1772–1779.
32. **Yang, L., T. M. Weiss, R. I. Lehrer, and H. W. Huang.** 2000. Crystallization of antimicrobial pores in membranes: magainin and protegrin. Biophys. J. **79:**2002–2009.
33. **Zasloff, M.** 2002. Antimicrobial peptides of multicellular organisms. Nature **415:**389–395.